Cell Metabolism
Resource

A Fluorescent Reporter of AMPK Activity and Cellular Energy Stress

Peiling Tsou,[1,2] Bin Zheng,[1,2,4] Chia-Hsien Hsu,[3,5] Atsuo T. Sasaki,[1,2] and Lewis C. Cantley[1,2,*]
[1]Department of Systems Biology, Harvard Medical School, Boston, MA 02115, USA
[2]Division of Signal Transduction, Beth Israel Deaconess Medical Center, Boston, MA 02115, USA
[3]BioMEMS Resource Center, Center for Engineering in Medicine and Surgical Services, Massachusetts General Hospital, Harvard Medical School, Boston, MA 02114, USA
[4]Present address: Department of Dermatology and Department of Pathology and Cell Biology, Institute for Cancer Genetics, Columbia University Medical Center, New York, NY 10032, USA
[5]Present address: Division of Medical Engineering Research, National Health Research Institutes, Miaoli 35053, Taiwan, Republic of China
*Correspondence: lewis_cantley@hms.harvard.edu
DOI 10.1016/j.cmet.2011.03.006

SUMMARY

AMP-activated protein kinase (AMPK) is activated when the AMP/ATP ratio in cells is elevated due to energy stress. Here, we describe a biosensor, AMPKAR, that exhibits enhanced fluorescence resonance energy transfer (FRET) in response to phosphorylation by AMPK, allowing spatiotemporal monitoring of AMPK activity in single cells. We show that this reporter responds to a variety of stimuli that are known to induce energy stress and that the response is dependent on AMPK α1 and α2 and on the upstream kinase LKB1. Interestingly, we found that AMPK activation is confined to the cytosol in response to energy stress but can be observed in both the cytosol and nucleus in response to calcium elevation. Finally, using this probe with U2OS cells in a microfluidic device, we observed a very high cell-to-cell variability in the amplitude and time course of AMPK activation and recovery in response to pulses of glucose deprivation.

INTRODUCTION

AMP-activated protein kinase (AMPK), an evolutionarily conserved metabolic gauge, serves as an energy stress sensor and a homeostatic regulator of cellular ATP levels (Hardie, 2007; Kahn et al., 2005; Lage et al., 2008; Steinberg and Kemp, 2009). This serine/threonine protein kinase exists as a heterotrimeric complex consisting of a catalytic α subunit and regulatory β and γ subunits each encoded by multiple genes (Stapleton et al., 1996; Woods et al., 1996). Recent studies have identified LKB1 and Ca^{2+}/calmodulin-dependent protein kinase kinase-beta (CaMKKβ) as upstream kinases that phosphorylate Thr-172 in the activation loop of the catalytic subunit to activate AMPK (Hawley et al., 2005; Hurley et al., 2005; Shaw et al., 2004; Woods et al., 2005). It has been proposed that the AMP binding to the regulatory γ subunit enhances phosphorylation by LKB1 while cellular calcium levels affect CaMKKβ dependent phosphorylation (Hawley et al., 2005; Hurley et al., 2005; Woods et al., 2005; Woods et al., 2003). Recently, Oakhill et al. have elegantly demonstrated that AMP directly stimulates α-Thr172 phosphorylation provided the AMPK β-subunit is myristoylated (Oakhill et al., 2010). AMP binding to AMPK also renders it less susceptible to dephosphorylation at Thr-172 by protein phosphatases (Sanders et al., 2007; Suter et al., 2006). Once activated, AMPK stimulates catabolic pathways that generate ATP, while inhibiting ATP-consuming processes such as biosynthesis and cell growth and proliferation (Hardie, 2007; Kahn et al., 2005).

Recently AMPK has been shown to play a central role in the regulation of body weight, systemic glucose homeostasis, lipid metabolism, and mitochondrial biogenesis, thus making it an attractive therapeutic target (Fogarty and Hardie, 2010; Kahn et al., 2005). In addition, AMPK also plays a crucial role in inhibiting many processes important for tumor development, including cell-cycle progression, protein synthesis, and cell growth, suggesting that AMPK activators could be used to prevent or treat cancers (Fay et al., 2009) (Engelman and Cantley, 2010).

In order to monitor the activation state of AMPK in cells and tissues, antibodies have been raised against phosphopeptides based on the sequence around Thr-172 of AMPK-α. These antibodies, along with antibodies that specifically recognize phosphorylated states of AMPK substrates, have been valuable for monitoring AMPK in western blots following cell lysis. However, current biochemical techniques do not allow for the measurement of AMPK signaling in real time in live cells. As a consequence, little is known about the location of AMPK activation in response to various stimuli or about the single-cell variability in AMPK activation. These questions are important since the upstream activator LKB1 can, under certain conditions, localize in the nucleus (Dorfman and Macara, 2008) and since some AMPK substrates are involved in gene regulation (McGee and Hargreaves, 2008; Shaw et al., 2005).

Here, we describe the design and application of an AMPK activity reporter (AMPKAR). Using AMPKAR, we were able to detect endogenous AMPK activity in real time in live cells. This reporter reveals differences in the subcellular localization, as well as temporal dynamics of AMPK activation through two different upstream kinases, LKB1 and CaMKKβ. Interestingly,

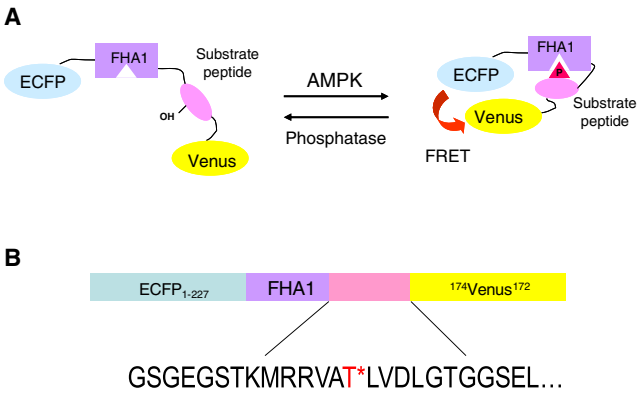

Figure 1. Schematic Representation of AMPKAR Construct

(A) Phosphorylation of the optimized AMPK substrate motif on AMPKAR induces binding to the intrinsic FHA domain, thereby prompting a conformational change that is detected by a change in fluorescence resonance energy transfer (FRET) between eCFP and an YFP variant Venus.

(B) Domain structures of AMPKAR and amino acid sequence of the optimized AMPK substrate motif.

using this probe, we also observed cell-cell variations in response to energy stress. We found that there was a wide variation in the response of individual U2OS cells to acute "hypoglycemia" (3 mM glucose), from no activation to near maximal activation and that in a given cell the time course and magnitude of responses to multiple pulses of "hypoglycemia" were highly conserved.

RESULTS

Design of the AMPK Activity Reporter

In order to monitor AMPK activity in living cells, we have designed a genetically encoded fluorescent reporter, AMPKAR, which is activated in response to phosphorylation by AMPK. AMPKAR was constructed analogously to a previously reported protein kinase A reporter, AKAR3 (Allen and Zhang, 2006). To produce an AMPK reporter, the AKAR3 template was modified within its substrate phosphorylation sequence in order to create a site optimized for both the favorable substrate motif for AMPK obtained from a positional scanning peptide library screen (Turk et al., 2006) and its subsequent recognition by the phosphothreonine-binding domain FHA1 (forkhead-associated domain1) from the yeast rad53p protein (Durocher et al., 2000). Our positional scanning peptide library approach revealed that AMPK has a strong selection for Leu at +4, Met or Leu at −5, and for Arg at −3 or −4. We avoided using Leu at −5 to reduce the possibility that the site would be phosphorylated by protein kinase D family members (which have a similar selectivity to AMPK but prefer Leu over Met at −5) (Hutti et al., 2004). After testing multiple versions of candidate motif sequences, MLRVATLVDL, MLRVASLVDL, MLRNATLVDL, MLHRATLVDL, and MRRVASLVDL (data not shown), we observed an optimal dynamic range of response using the motif MRRVATLVDL. The resulting AMPKAR reporter protein consists of the FRET pair eCFP and circularly permuted variants of Venus cpV E172 (Nagai et al., 2004), bracketing an FHA1 domain and an AMPK substrate motif (Figure 1). Phosphorylation of the AMPK substrate within the reporter drives its binding to the FHA1 module resulting in the juxtaposition between the donor (eCFP) and acceptor (YFP variant Venus) fluorophores resulting in fluorescence resonance transfer (FRET).

AMPKAR Reports Endogenous AMPK Activity in Live Cells

To test whether AMPKAR is able to report endogenous AMPK activation, we expressed AMPKAR in COS-7 cells and monitored the FRET ratio change after addition of 20 mM 2-deoxyglucose (2-DG), a glucose analog that inhibits glycolysis and lowers ATP levels. During the first couple of minutes after 2-DG addition, there was a sharp decline in the FRET ratio (Figure 2A), presumably due to a change in osmolarity (a similar drop in FRET ratio occurs upon adding L-glucose [Figure S1 available online] and was also observed when the substrate peptide phosphorylation site was mutated from threonine to alanine [Figure 2C]). After the decline, we detected a gradual and steady increase in FRET signal that reached a maximum (17.9% ± 1.5%, average ± standard error, n = 32) approximately 15 min after 2-DG addition. Isoelectric focusing of AMPKAR indicates that a 20% increase in FRET correlates with about 40% phosphorylation (data not shown). The response observed with our AMPK sensor was consistent with results obtained in parallel experiments with western blot analysis with antibodies directed against the known cellular AMPK substrate, phosphoserine 79 in Acetyl-CoA carboxylase (pACC Ser79), as well as with high-performance liquid chromatography (HPLC) measurement of intracellular AMP:ATP ratio, as shown in Figure 2B and Figure S2, respectively.

Phosphorylation of AMPK on Thr-172 leads to its activation and is catalyzed by at least two distinct upstream kinases, the tumor suppressor LKB1 (Shaw et al., 2004; Woods et al., 2003) and CaMKKβ (Hawley et al., 2005; Hurley et al., 2005; Woods et al., 2005). To test whether AMPKAR can report signals mediated via CaMKKβ, we treated AMPKAR expressing Cos-7 cells with the calcium ionophore ionomycin. As shown in Figure 2B, treatment with ionomycin resulted in a maximal response (37.8% ± 2.2%, n = 15) within 3 min. The AMPKAR- FRET response to ionomycin was more rapid and transient than that observed after 2-DG stimulation. These results were consistent with those of parallel western blot analysis with antibodies directed against pACC Ser79.

Interestingly, we observed differences in the location of AMPK activation in response to 2-DG versus ionomycin. As shown in Figure 2A, the activation in response to 2-DG occurred within the cytosol, mainly within the perinuclear region. In contrast, calcium ionophore elicited activation was more widespread (Figure 2B).

AMPKAR FRET Responses Are Specific to AMPK

To determine whether the production of the FRET signal in response to AMPK activators was due to phosphorylation at the threonine within the AMPK substrate motif site, we mutated this residue to an alanine and tested the response of mutant AMPKAR-T/A. COS-7 expressing AMPKAR-T/A did not show a change in the FRET signal in response to either 20 mM 2-DG or 1 μM ionomycin (Figure 2C), suggesting that the observed change in the FRET signal indeed results from phosphorylation at the designed AMPK phosphorylation site.

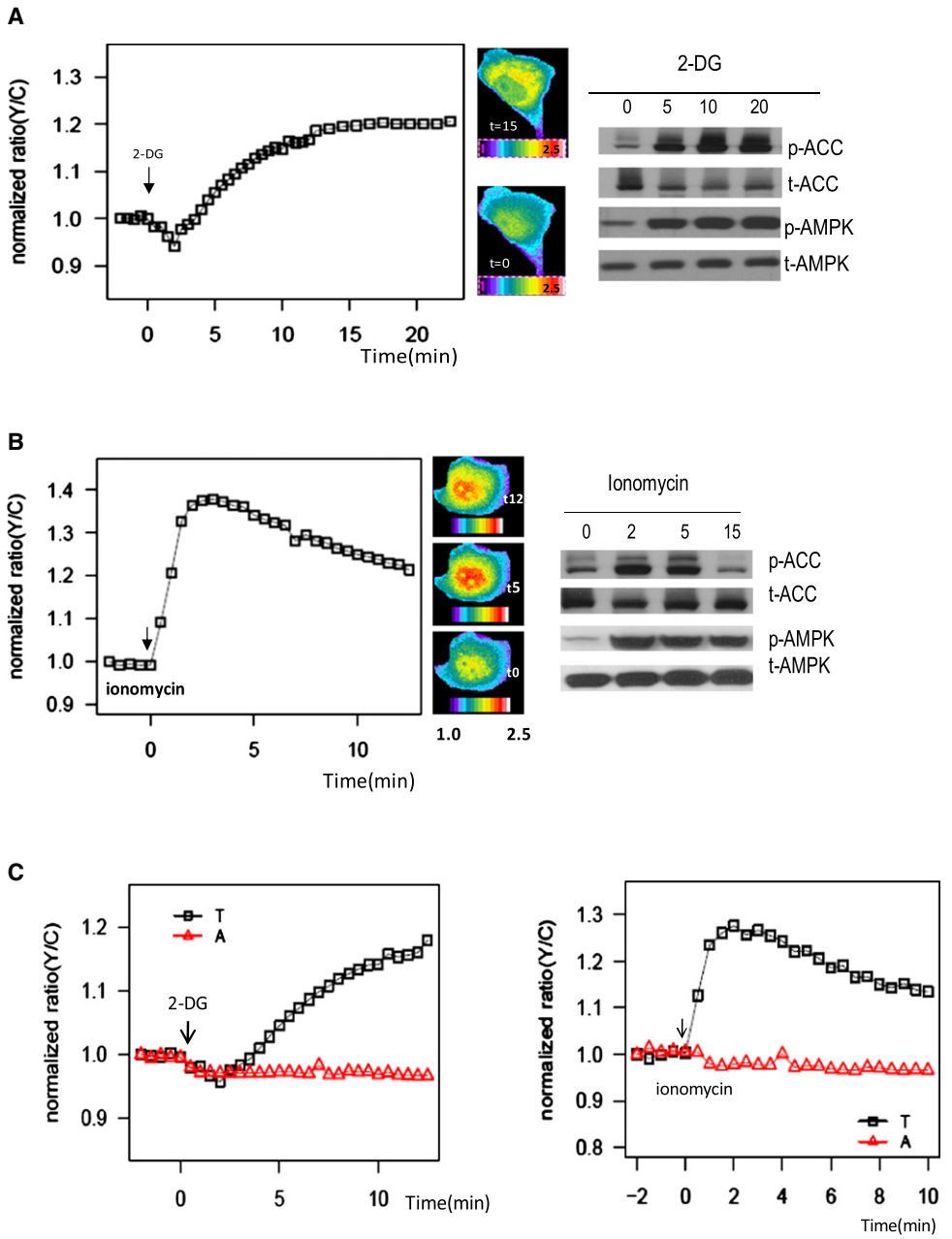

Figure 2. AMPKAR FRET Response to Energy Stress and Calcium Elevation

(A) COS-7 cells expressing AMPKAR were treated with 20 mM 2-DG. Left: mean normalized (Y/C) emission ratio (n = 32). Middle: representative pseudocolor images of Y/C ratio show the FRET response. Right: western blots showed comparable time course for AMPK activation indicated by an increase in phospho-ACC (S-79) and the corresponding phospho-AMPK (T-172) levels.

(B) COS-7 cells transfected with AMPKAR were treated with 1 μM ionomycin. Left: mean normalized (Y/C) emission ratio (n = 15). Middle: representative pseudocolor images of Y/C ratio show the FRET response. Right: western blots showed comparable time course for AMPK activation indicated by increase of phospho-ACC (S-79) and the corresponding phospho-AMPK (T-172) levels.

(C) T to A mutation in the substrate peptide phosphorylation site abolishes FRET. Left: COS-7 cells expressing either AMPKAR(T) (n = 30) or mutant AMPKAR(A) (n = 8) were treated with 20 mM 2-DG. Right: Cos-7 cells expressing either AMPKAR(T) (n = 14) or mutant AMPKAR(A) (n = 18) were treated with 1 μM ionomycin.

Considering the similarity among the optimal substrate motifs of PKA, PKC, PKD, and AMPK family members, next we examined whether activation of PKA, PKC, or PKD would cause any signal changes detected by AMPKAR. COS-7 cells expressing either AMPKAR or a reporter for protein kinase D (DKAR) (Kunkel et al., 2007) or a reporter for PKA (AKAR3) (Allen and Zhang, 2006) were stimulated with 200 nM phorbol myristate acetate (PMA) to activate PKC and PKD family members or 50 μM forskolin to activate PKA, and FRET responses were monitored. DKAR undergoes a decrease in FRET signal in response to

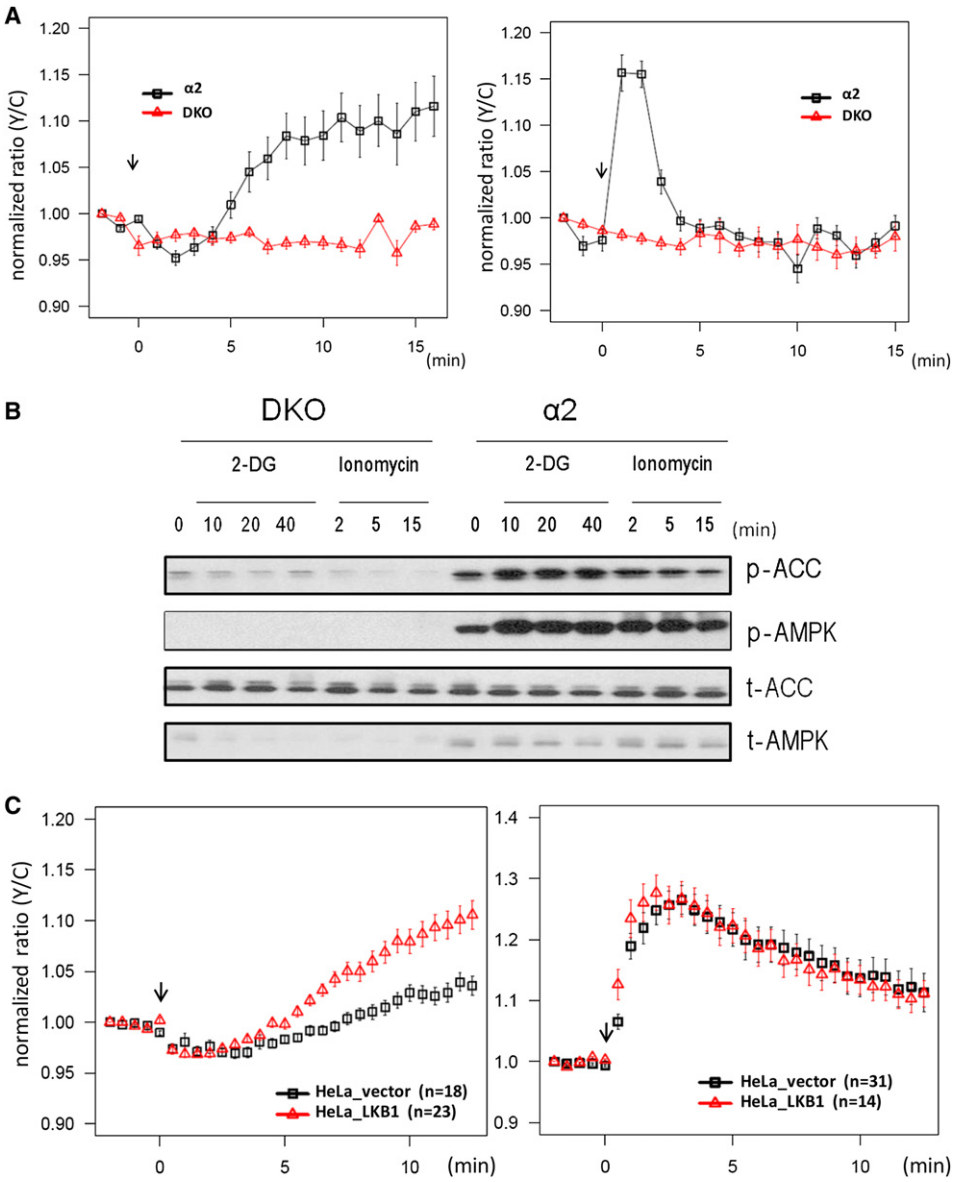

Figure 3. AMPKAR FRET Signal Is AMPK Dependent

(A) The AMPKAR FRET response is not observed in mouse embryonic fibroblasts that lack AMPK. MEFs lacking both AMPK-α1 and α2 (DKO) or DKO cells reconstituted with AMPK α2 subunit (α2) were treated with either 20 mM 2-DG (left) (DKO, n = 6; a2, n = 11) or 1 μM ionomycin (right) (DKO, n = 4; α2, n = 13). Data are presented as mean ± standard error. All drugs were added at time zero.

(B) Western blots of DKO versus α2 MEF treated under the same conditions as those used in the imaging experiments.

(C) The AMPKAR FRET response to energy stress requires LKB1. AMPKAR FRET signals were compared between HeLa cells reconstituted with LKB1 (HeLa_LKB1) or vector (HeLa_vector). Cells were treated with either 20 mM 2-DG or 1 μM ionomycin. Data are presented as mean ± standard error.

phosphorylation by protein kinase D and, as shown in Figures S3A and S3B, cells expressing DKAR exhibited a decrease in FRET when treated with PMA, consistent with PKD activation. Cells expressing AKAR3 exhibited an increase in FRET in response to forskolin, consistent with PKA activation. However, neither PMA nor forskolin induced a FRET response in cells expressing AMPKAR. These results indicate that AMPKAR is not an in vivo substrate for PKA, PKC, or PKD family members.

To determine whether the AMPKAR FRET response requires AMPK, we used mouse embryonic fibroblasts (MEFs) derived from AMPK knockout mice (Laderoute et al., 2006). We expressed AMPKAR in AMPK α1 and α2 double knockout (DKO) MEFs or in DKO MEFs in which the α2 subunit (α2) of AMPK had been reintroduced (Figures 3A and 3B). As expected, western blots revealed that phosphorylation of ACC and AMPK in response to either 2-DG or the calcium ionophore, ionomycin were observed in reconstituted α2 MEFs (α2) but not in AMPK DKO cells. Likewise, the AMPKAR-FRET signal change was detected in AMPK α2 reconstituted MEFs but not in DKO MEFs. Taken together, these results strongly indicate that AMPKAR is

a selective reporter of AMPK activity under these stimulation conditions.

We next asked whether the AMPKAR FRET response to 2-DG and ionomycin are dependent on the expected upstream kinases. LKB1 has been shown to be required for activation of AMPK in response to 2-DG and other agents that lower the ATP/AMP ratio, while CaMKKβ has been shown to mediate calcium-dependent activation of AMPK. We expressed AMPKAR in HeLa cells, which are deficient in LKB1 and found that the FRET response to ionomycin was maintained, but that the response to 2-DG was defective (Figure 3C). Expression of LKB1 in HeLa cells restored the AMPKAR FRET response to 2-DG but had no effect on the response to ionomycin. These results further validate AMPKAR as an in vivo AMPK response indicator.

Characterization of Subcellular AMPK Activity

Next, we were interested in determining whether AMPKAR could be used to monitor AMPK activity in distinct cellular compartments. To measure AMPK activity exclusively in the cytosol or nucleus, we attached either a nuclear export signal (NES) or nuclear localization signal (NLS), respectively, to the C terminus of AMPKAR (Figure 4A). The NES-tagged reporter localized to the cytosol and the NLS-tagged reporter localized to the nucleus, as expected. Addition of 1 μM ionomycin induced a FRET response in both NES- and NLS-tagged AMPKARs, and, interestingly, the cytosolic response from NES-tagged AMPKAR was of greater magnitude (32.8% ± 1.9%, n = 20 versus 20% ± 2.0%, n = 27) and occurred more rapidly (time to reach 50% maximal response of <1 min versus 2.5 min) (Figure 4B). The AMPKAR-FRET signal changes elicited from addition of either 20 mM 2-DG or 2 mM AICAR were almost exclusively confined to the cytosolic compartment (Figures 4C and 4D). This interesting observation is in agreement with previous reports showing that LKB1 activation takes place predominantly in the cytoplasm, after it complexes with STRAD (STE-related adaptor) and MO25 (mouse protein 25) (Boudeau et al., 2003; Dorfman and Macara, 2008; Hawley et al., 2003).

AMPKAR Senses Intracellular Energy Stress in a Timely and Reversibly Fashion

We next examined whether AMPKAR can reversibly and dynamically report the energy status of living cells in response to a more physiological or pathophysiological alteration in nutrient availability. To address this question, we designed a microfluidic cell culture system (Figure S4) to examine AMPKAR signals in real time in response to altered extracellular glucose.

COS-7 cells expressing either AMPKAR or an intracellular glucose reporter, FLII12Pglu-700uDelta6 (Takanaga et al., 2008), were cultured in microfluidic channels and a controlled flow of DMEM media with a varied glucose concentration was passed over the cells. Interestingly, cells responded rapidly to alterations in extracellular glucose concentration. As shown in Figure 5, when the glucose concentration in the medium dropped from 25 mM to 0 mM, the signal change from the intracellular glucose sensor was detectable within 1 min and reached a plateau in less than 3 min (20.0% ± 3.4%, n = 10). Notably, the AMPKAR FRET signal increased rapidly with only about a 1 min lag after the drop in cellular glucose. When the glucose in the medium was restored to 25 mM, cellular glucose levels returned to normal within approximately 5 min and the AMPKAR FRET signal dropped to basal level with only a slight lag. These results indicate that in these cells, cytosolic glucose levels and ATP/AMP ratios (as judged by AMPK activity) are dynamically controlled by extracellular glucose. These results also indicate that AMPKAR is rapidly dephosphorylated when AMPK activity drops.

AMPKAR Reveals the Similarity and the Variation of Cellular Energy Stress Responses

Heterogeneity among individual cells is a common feature of dynamic cellular processes. To better understand how heterogeneity contributes to the overall tissue level phenotype, it is important to know which properties of the response vary from cell to cell and which are robust between cells (Spencer et al., 2009). Using U2OS cells stably expressing AMPKAR, we examined cell variability in AMPK activation in response to energy stress. Energy stress was induced with a microfluidics device to cause an acute change in glucose from 25 mM in normal media to either 0 mM or 3 mM (Figure S4). In response to complete withdrawal of glucose, all the cells examined exhibited an increase in the AMPKAR FRET signal, though the half time for response and magnitude of response was variable from cell to cell (Figure 6A). When glucose was replenished by switching back to regular media with 25 mM glucose, the signal promptly returned to basal level. When treated with a second pulse of 0 glucose, each cell responded in a similar fashion to the first pulse.

When cells were shifted from 25 mM glucose to a more physiologically relevant level of "hypoglycemia" (3 mM glucose) there was a greater cell-to-cell variability AMPKAR FRET response. Twenty-three percent (six out of 26) of the cells failed to respond to this more modest stress, while a few cells showed a near maximum response (Figure 6B). Interestingly, all cells that responded to the first pulse also responded to the second pulse. No increase in AMPKAR FRET signal was observed in the control channel, in which cells were perfused with medium with a constant 25 mM glucose concentration.

To quantify the variability in the dynamics, we measured several parameters of the response profile to both pulses of glucose starvation for each cell, including the half times for the increase ($T_{1/2}up_1$,$T_{1/2}up_2$) and decrease ($T_{1/2}d_1$,$T_{1/2}d_2$) phases for each pulse, and the maximal response amplitude (Amp_{Max1},Amp_{Max2}); see Figure 6C for definitions. To measure cell-cell variability, we used the coefficient of variation (CV), defined by the ratio of the standard deviation to the mean (CV = SD/mean), as shown in Figure 6D.

When cells were exposed to modest stress with physiologically relevant "hypoglycemia" with 3 mM glucose, the maximal amplitude (Amp_{Max}) of response showed a large variation among cells (CV = 64%–69%). In contrast, two of the temporal parameters showed relatively modest cell-cell variability: around 16%–20% in $T_{1/2}$ up and 20%–25% in $T_{1/2}$ d.

In response to complete glucose withdrawal, there was less variability in these parameters (Figure 6D). Not surprisingly, cells responded faster (mean ± SE: $T_{1/2}$ up_1: 4.12 ± 0.20 min versus 4.84 ± 0.22 min, p = 0.02) and more strongly (Amp_{Max}: 31.0% ± 1.9% versus 11.8% ± 1.4%, p = 6.88E–10) to harsh stress (zero glucose) than to modest stress (glucose 3 mM).

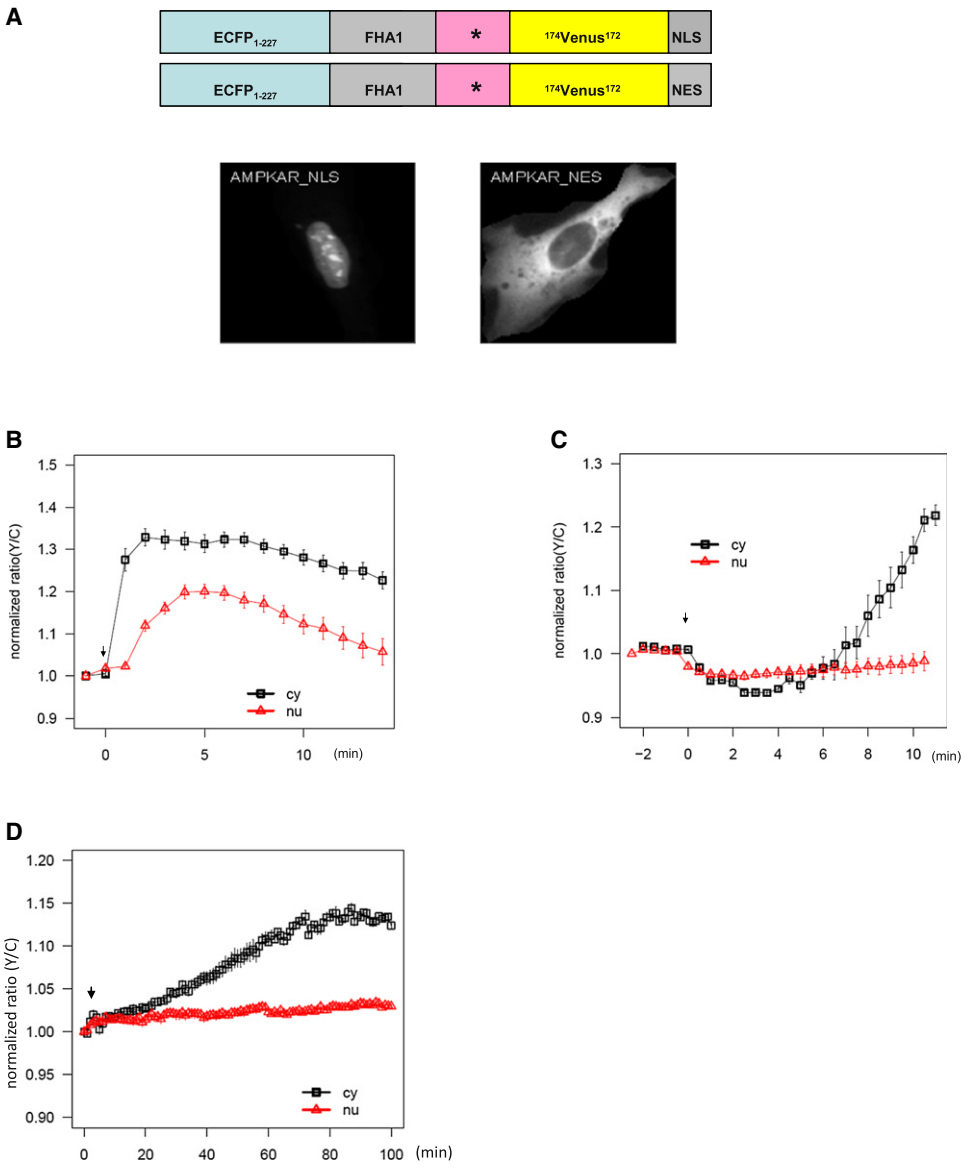

Figure 4. Subcellular Targeting of AMPKAR

(A) Schematic domain structures of nuclear and cytosol targeted AMPKAR. The asterisk represents the localization of the AMPK substrate motif. YFP fluorescence image of AMPKAR-NLS (left) or AMPKAR-NES expressing C2C12 cells.

(B) Representative emission ratio time course of cytosolic (cy, n = 20) versus nuclear targeted AMPKAR in response to 1 μM ionomycin (nu, n = 27). Data are presented as mean ± standard error.

(C) Representative emission ratio time course of cytosolic (cy, n = 5) versus nuclear (nu, n = 16) targeted AMPKAR in response to 20 mM 2-DG treatment. Data are presented as mean ± standard error.

(D) Representative emission ratio time course of cytosolic (cy, n = 6) versus nuclear (nu, n = 19) targeted AMPKAR in response to 1 mM AICAR treatment. Data are presented as mean ± standard error. All drugs were added at time 0 as indicated by arrows.

However, there was no significant difference in the recovery time for the two stresses ($T_{1/2}$ d 2.82 ± 0.15 min versus 2.81 ± 0.16 min, p = 0.96). Importantly, comparing cellular responses of two episodes of stimulation from the same strength of stress, we found that there is no significant difference between the two pulses in either the amplitude or the time parameters (Figure 6E), suggesting that on this time scale, the cell characteristics that provide the variability in homeostatic response to glucose withdrawal do not significantly change.

DISCUSSION

The fluorescent biosensor AMPKAR presented here represents a novel tool for monitoring AMPK activity in living cells. In comparison with the existing methods for measuring AMPK activation, AMPKAR offers many advantages. It provides information that is consistent with biochemical approaches, yet with greater spatiotemporal resolution at both the single cell and cell population levels. We showed that the enhanced

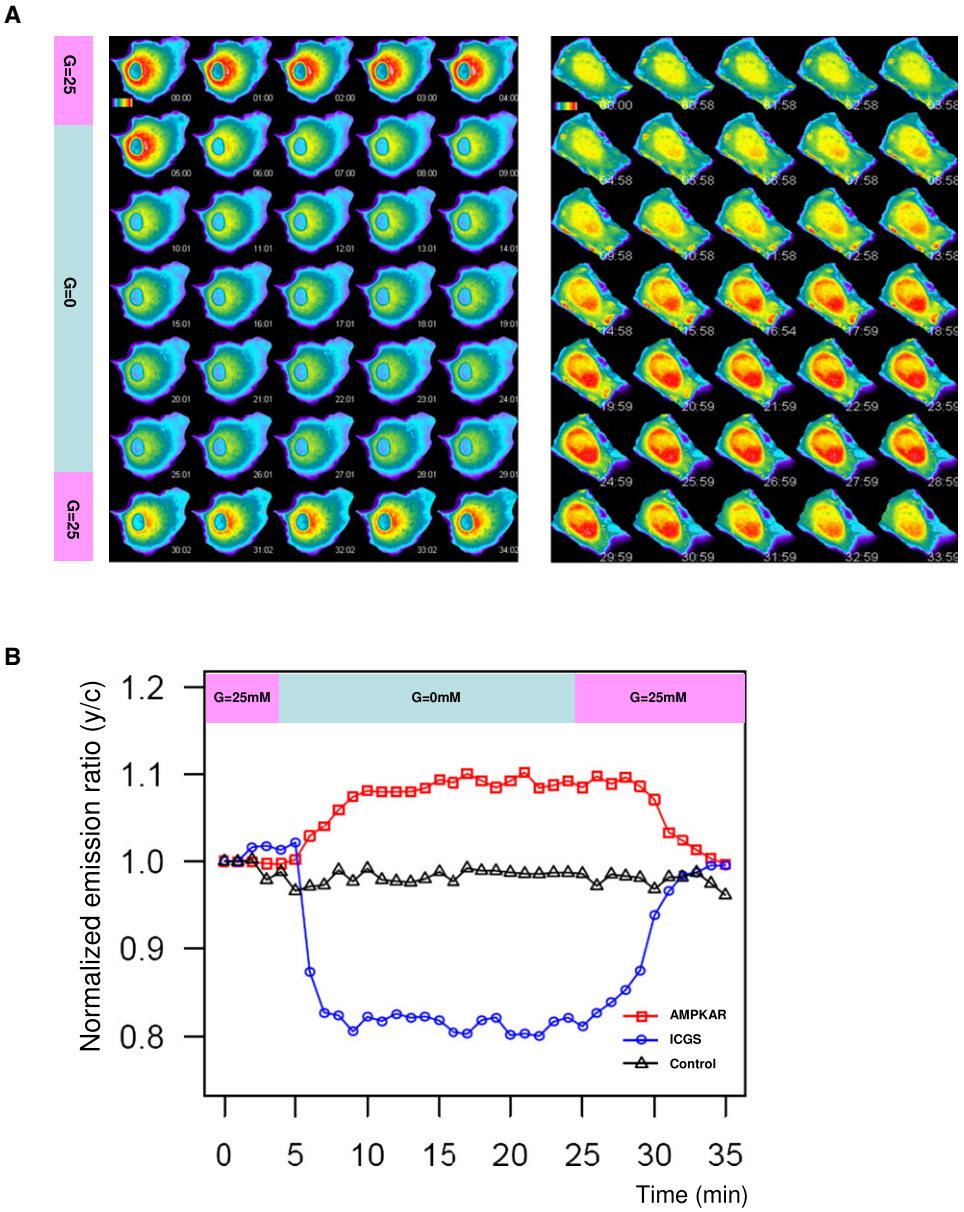

Figure 5. AMPKAR Exhibits Reversible Dynamics

(A) Manipulating extracellular glucose concentrations leads to reciprocal changes of FRET signals from AMPKAR and ICGS (intracellular glucose sensor FLII12Pglu-700uDelta6). COS-7 cells were transfected with either AMPKAR (right) or ICGS (left) and seeded on the microfluidic devices. Cells were perfused with a continuous flow of regular DMEM with 25 mM glucose for 4 min (time points 1–5), switched to glucose free DMEM (G = 0) for 20 min, and then switched back to regular DMEM with 25 mM glucose (G = 25). Each frame shows the FRET ratio at 1 min intervals (left to right and top to bottom).

(B) Tracings of the AMPKAR FRET response (squares; average from 30 cells) and ICGS FRET response (circles; average from ten cells) from cells treated as described in (A). The AMPKAR FRET signal from the control in which cells were continuously exposed to a flow of 25 mM glucose throughout the time course is also presented (triangles; averaged from seven cells).

AMPKAR FRET signal in response to energy stress or cytosolic calcium elevation depends on the presence of AMPK in the cell, indicating that AMPKAR is a good reporter of AMPK activity in responses to these stimuli. We also showed that AMPKAR does not respond to stimuli that activate PKA, PKC, and PKD family members. It is possible that AMPKAR is phosphorylated by the MARK (microtubule affinity-regulating kinase) family of protein kinases, which are closely related to AMPK. Our studies indicate that in response to energy stress or calcium elevation, the AMPKAR FRET signal is dependent on AMPK activation. Future studies should reveal whether stimuli that activate any other signaling pathways including AMPK-related kinases can also induce an AMPKAR FRET response.

AMPKAR was not only capable of capturing the dynamics of AMPK activity in real time but also demonstrated spatial variations in activity elicited by different stimuli. AMPK, its upstream

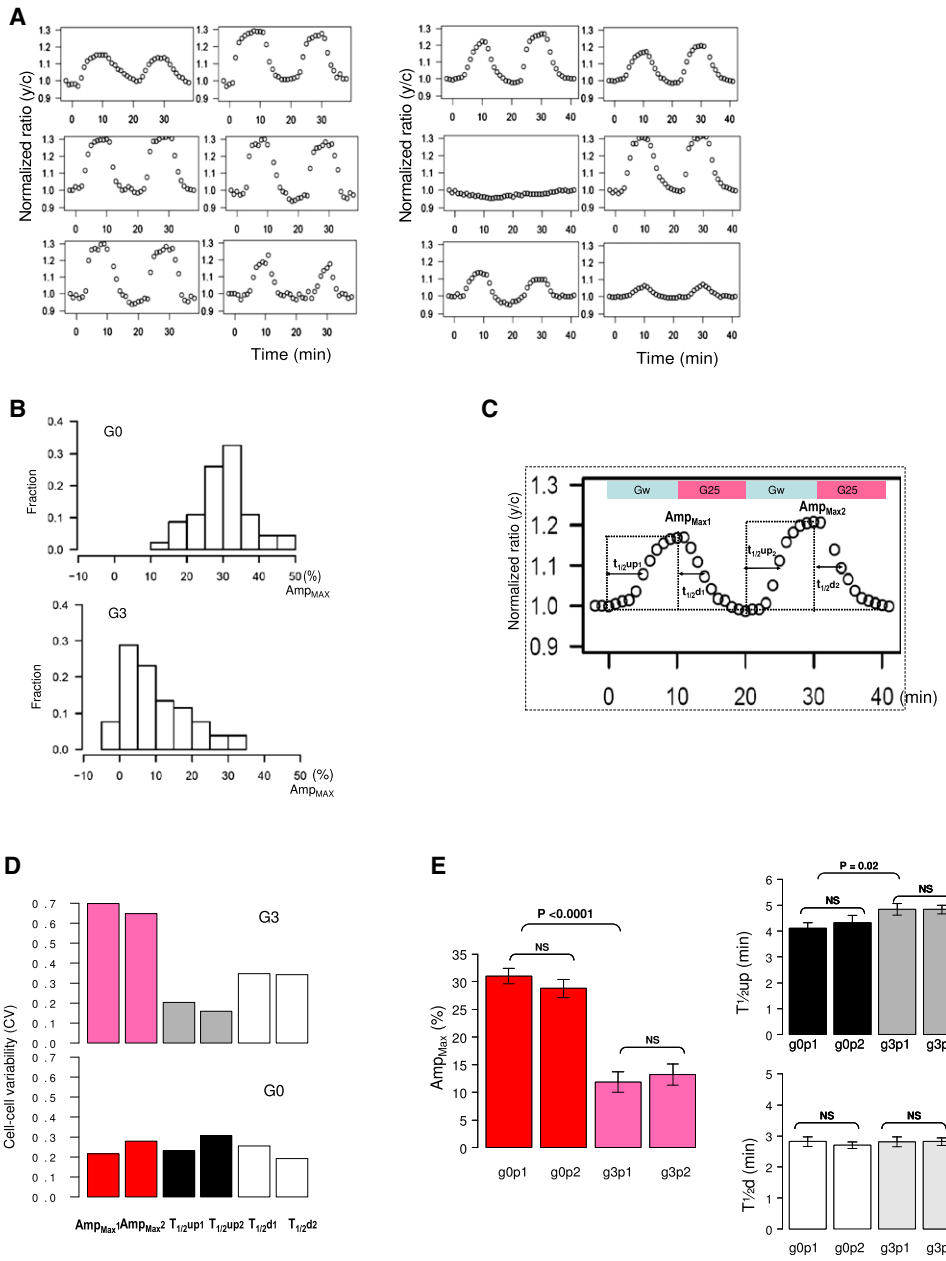

Figure 6. AMPKAR Reveals Cell-to-Cell Variability in Energy Stress Response

(A) AMPKAR reveals cell-cell variations in energy stress response. At time 0, U2OS cells stably expressing AMPKAR were switched from media with 25 mM glucose to media with either 0 glucose (six boxes on left) or 3 mM glucose (six boxes on right). After 10 min, the cells were shifted back to 25 mM glucose, at 20 min they were shifted back to the low glucose, and at 30 min they were shifted back to high glucose. The 12 boxes are representative single cell tracings of cellular FRET response to the two pulses of "low glucose."

(B) Distribution of maximal AMPKAR FRET response (Amp_{MAX}) from individual cells exposed to 0 (G0) or 3 mM glucose (G3).

(C) Definition of parameters in AMPKAR activity in response to low glucose stimulation. Gw denotes glucose withdrawal and G25 denotes 25 mM glucose in media. Amp_{Max} denotes the maximal FRET signal (normalized y/c ratio); $T_{1/2}$up denotes the time to reach half of maximal response (minutes), $T_{1/2}$d denotes the time to return to half of maximal fluorescence during FRET decrease (minutes). Subscript 1 and 2 denotes response from first and second pulses, respectively.

(D) Cell-cell variability measured as the CV (coefficients of variance: ratio of standard deviation to mean) of different aspects of cellular response to glucose starvation. Top: AMPKAR FRET response upon shift to 3 mM glucose (G3). Bottom: AMPKAR FRET response upon shift to zero glucose (G0).

(E) While the median increase in the AMPKAR FRET amplitude is greater upon complete glucose removal compared to partial glucose removal, cells exhibit a similar response in the second pulse of low glucose to the response in the first pulse, and the half times for the increase and decrease of the FRET signal are relatively constant. Data are presented as mean ± standard error. g0 denotes zero glucose; g3 denotes 3mM glucose; p1 and p2 denote first and second pulses of stimulation, respectively. (NS, statistically nonsignificant.)

activating kinases and downstream substrates may preferentially reside in distinct subcellular compartments. Targeting AMPKAR to the nucleus or cytosol provides a readout of AMPK activity in these locations, and thus facilitates the detection of a spatial-specific role of AMPK in signal propagation. For example, AMPK has been reported to control a number of transcriptional processes as well as epigenetic events (McGee and Hargreaves, 2008); however, how nuclear AMPK itself is activated has remained unclear. When we activated AMPK by the energy stress inducing agent 2-DG, or the AMP mimetic AICAR, we observed that AMPK activation by LKB1 is largely localized to the cytosol. In contrast, ionomycin-induced AMPK activation (presumably mediated by CaMKKβ) occurred both in the cytosol and nucleus. While it has been shown that LKB1 activation takes place predominantly in the cytoplasm, after it complexes with STRAD and MO25 (Boudeau et al., 2003; Dorfman and Macara, 2008; Hawley et al., 2003), it is still possible that AMPK is activated in the nucleus under certain conditions since LKB1 can shuttle between the cytoplasm and the nucleus (Dorfman and Macara, 2008). Further studies will be necessary to determine under what conditions, if any, AMPK becomes activated in the nucleus in response to energy stress.

Signaling cascades propagate information about fluctuations in the extracellular environment so that cells can respond accordingly. As an energy sensor, how does AMPK sense and react to relevant stimuli that encode information about a fluctuating environment? Taking advantage of microfluidic technology in combination with AMPKAR, we were able to visualize rapid and reversible cellular responses to the alterations of extracellular glucose and to ask whether individual cells respond differently to energy stress. We observed that, under modest energy stress, the timing of response is less variable than the amplitude of response. This is intriguing since similar results have previously been reported in other systems, including the ERK response to EGF (Cohen-Saidon et al., 2009), in p53 oscillations (Geva-Zatorsky et al., 2006), and circadian oscillations (Mihalcescu et al., 2004). When stress is more severe, however, cellular responses become faster and stronger, and the cell-to-cell variations also are smaller. Despite the variability, we also found that some aspects of the dynamics upon energy stress are very similar between cells: both the magnitude of response and the response time are related to the level of the stimuli. Notably, most cells return to their original basal levels after an initial pulse, and the peak heights as well as the time to reach maximal response are similar in two sequential pulses. This kind of adaptation behavior could be crucial for AMPK as an energy stress sensor, allowing it to reset itself and become ready to respond to the next stimulus in a dynamically changing environment.

During the development of CFP-YFP-based FRET reporters for adenosine nucleotides, Willemse et al. reported that all of their FRET constructs had a significant response to millimolar levels of ATP (Willemse et al., 2007). As the authors pointed out, this is a cautionary note for ATP interference with all FRET-based sensors. In the scenario of AMPKAR, it is unlikely that the signal change we observed was due to dequenching of the FRET signal resulting from the decrease in ATP levels, since the FRET signal was abolished when we mutated the substrate site threonine of AMPKAR to an alanine and was also abolished upon deletion of both AMPK genes.

In summary, we have designed and characterized a genetically encoded FRET based biosensor, AMPKAR, to provide a selective, reversible, and real-time readout of AMPK activity. This tool offers an opportunity to probe both when and where AMPK is activated in living cells/tissues, and possibly living animals, during physiological or pathological conditions. It might also facilitate AMPK activator drug discovery in high-content screening. Furthermore, this AMPK response reporter provides new insight into single cell responses to energy stress that will be valuable for understanding energy homeostasis.

EXPERIMENTAL PROCEDURES

Materials

Anti-phospho-AMPK (Thr172), anti-AMPK, anti-phospho-ACC and anti-ACC antibodies were purchased from Cell Signaling Technology. AICAR was obtained from Toronto Research Chemicals (Downsview, ON, Canada). 2-DG and ionomycin were purchased from Sigma and Cell Signaling Technology, respectively. AKAR3 and DKAR plasmids were kindly provided by Jin Zhang and Alexandra Newton, respectively. Intracellular glucose concentration reporter (FLII12Pglu-700uDelta6) was obtained from Addgene (contributed by Wolf Frommer Laboratory).

AMPKAR Construction

AMPKAR was engineered by starting with the sequence of the PKA reporter, AKAR3 and modifying the substrate motif to be optimal for AMPK, based on previous studies with peptide libraries. Several versions of the substrate sequence were generated, including MLRVATLVDL, MLRVASLVDL, MLRNATLVDL, MLHRATLVDL, MRRVATLVDL, MRRVASLVDL, and MRRVAALVDL (T/A mutant) by PCR mutagenesis with QuikChange protocol (Stratagene). For cytosolic targeting, NES PKKKRKVEDA (Zhang et al., 2001) was added to the C terminus of Venus in the AMPKAR construct. For nuclear targeting, three tandem repeats of the SV-40 large T antigen NLS peptide DPKKKRKV were fused to the C terminus of Venus. All constructs were verified by sequencing after subcloning into the pcDNA3.1 vector.

Cell Culture, Transfection, and Generation of Stable Cell Lines

COS-7, C2C12, HeLa cells were maintained in Dulbecco's modified Eagle's medium (DMEM; GIBCO) containing 10% fetal bovine serum and 1% penicillin/streptomycin at 37°C in 5% CO_2. For retroviral transfection, amphotropic retrovirus were generated as described previously (Zheng and Cantley, 2007). MEFs were maintained in DMEM containing 10% fetal bovine serum and 1% penicillin/streptomycin at 37°C in 10% CO_2. Cells were plated onto fibronectin coated MatTek dishes prior to transfection. Transient transfection was carried out using FuGENE 6 (Roche Diagnostics) for COS-7, HeLa, and C2C12 cells, and Lipofectamine LTX (Invitrogen) for MEFs. Imaging was carried out 18 to 36 hr after transfection. U2OS cells stably expressing AMPKAR were generated utilizing Gateway recombination cloning technology (Invitrogen). In brief, AMPKAR was cloned into a lentiviral vector engineered from a pHR backbone and CMV promoter. Lentiviruses were generated by cotransfecting each recombined destination vector with packaging plasmid (delta8.9), envelope protein plasmid (VSV-G) to HEK293T by Fugene 6 (Roche) as recommended by the manufacturer. Fresh medium was added to the cells 24 hr after transduction, and 2 μg/ml puromycin was added for selection. The medium was replaced every 3 days until foci could be identified, and individual foci were then selected and expanded.

Microfluidic Device Layout Design and Microfabrication

The microfluidic device was designed for rapid switch of the cell culture medium surrounding cultured cells. This device consists of five microfluidic channels in which cells were seeded and cultured under constant perfusion (600 μl/hr) of cell culture medium introduced from two inlets (as shown in Figure S4). After the cells attached to the substrate (~2–4 hr, depending on cell type), the medium from one inlet was replaced with a medium containing the desired stimuli to cultured cells. To selectively expose cells to the stimuli, the position of the interface where the two fluids meet, was adjusted by

changing the hydrostatic pressures used for driving the two fluids. For example, when the hydrostatic pressure driving the stimuli-containing medium from the right inlet is higher, the interface of the two fluids shifts to the left, cells in the third channel are exposed to regular medium (Figure S4B). On the other hand, when the hydrostatic pressure driving the stimuli-containing medium from the left inlet is higher, the interface of the two fluids shifts to the right, and glucose free medium flows to the cells in the third channel (Figure S4C). As a result, cells in each individual channels can be temporally exposed to the stimuli at will.

Our microfluidic devices were made of Polydimethylsiloxane (PDMS) (Sylgard 184, Dow Corning, Midland, MI) and glass with soft lithography techniques (McDonald et al., 2000). In brief, negative photoresist (SU-8, MicroChem, Newton, MA) was photolithographically patterned on a silicon wafer to create a master with microscale features. The heights of SU-8 features (90 μm) on the master were measured with a surface profilometer (Dektak ST System Profilometer, Veeco Instruments, Plainview NY). The master was then used as a mold, on which PDMS prepolymer mixed with its crosslinker at 10:1 weight ratio was poured, degassed, and allowed to cure in a conventional oven at 65°C for 24 hr. The cured PDMS replicas were removed from the mold, subjected to a brief oxygen plasma treatment, and bonded to glass substrates to form the final devices.

Glucose Perfusion

For the experiment demonstrating reciprocal change of intracellular glucose reporter and AMPKAR, cells were perfused with 25 mM glucose for 4 min (time points 1–5) at the beginning of the experiment to establish a baseline response. Then glucose-free media was perfused for 20 min to record the response from intracellular glucose concentration reporter (FLII12Pglu-700uDelta6) or the response from AMPKAR. Finally, glucose concentration was switched back to 25 mM for another 10 min. For the experiment of single cell response variations to glucose starvation, cells on the device were perfused with regular media containing 25 mM glucose initially as a baseline condition for 2 min (time points 0–3) and then switch to media containing either zero or 3 mM glucose for 10 min. Then, glucose was replenished by switching back to regular media with 25 mM glucose for another 10 min. A second pulse of "glucose starvation" was again administered, to test whether cells remain responsive to another episode of energy stress.

Live-Cell Imaging

Cells were plated on either number 1.5 coverslips MatTek Dish (#P35G-1.5-14-C) or microfluidic devices (see the Supplemental Experimental Procedures for details). DMEM media (GIBCO) containing 25 mM HEPES, 25 mM glucose (except for the experiment of manipulating glucose concentration), 2 mM glutamine, and 3% FBS, (phenol red was excluded during image acquisition). Cells were imaged on a Nikon TE 2000E and a Nikon and Ti motorized inverted microscope with 20×/0.75 or 60×/1.4 (oil immersion) NA objective lens. Dual emission ratio imaging was performed with a 436/10 filter, a diachronic mirror (Chroma 86002v1bs), and two emission filters (470/30 for cyan and 535/30 for yellow). All optical filters were obtained from Chroma Technologies. Images were acquired with a Hamamatsu ORCA-R2 cooled CCD camera controlled with MetaMorph 7 software (Molecular Devices) and the Perfect Focus System for continuous maintenance of focus. Fluorescence images were background-corrected. For time-lapse experiments, images were collected every 30–60 s, with an exposure time of 50–100 ms and 2×2 binning, with illumination light shuttered between acquisitions. The ratios of yellow-to-cyan were then calculated at different time points and normalized by dividing all ratios by the emission ratio before stimulation, setting the basal emission ratio as 1.

Western Blotting

Cell lysates were prepared with lysis buffer containing HEPES (pH 7.0), 150 mM NaCl, 1% NP-40, 1 mM EDTA, 50 mM NaF, 10 mM β-glycero-phosphate, 10 nM calyculin A, 1 mM Na_3VO4, and protease inhibitors and normalized by protein concentrations using the Bradford method (Bio-Rad). For western blotting, protein samples were separated on 8%–12% SDS-PAGE and transferred to PVDF membranes (Millipore). Membranes were blocked in TBST containing 5% nonfat milk, incubated with primary antibodies according to the antibody manufacturer's instructions, followed by incubation with horseradish peroxidase-conjugated goat anti-rabbit or anti-mouse IgG (Chemicon) and enhanced chemiluminescence detection (Perkin Elmer).

Measurement of ATP and AMP in 2DG-Treated COS7 Cells by HPLC

COS7 cells were treated with or without 2DG for the indicated time and lysed with 10% HClO4. The nucleotide-containing fraction was purified by mixed phase extraction employing 11.75:13.25 (vol/vol) of tri-n-octylamine (Sigma) and Freon 11 (Sigma). HPLC was performed as described previsouly (Budinger et al., 1996) with Agilent Technology 1200, a Zorbax Rx-C8 column (4 × 250 mm), buffer A; 50 mM KH2PO4, 8 mM tetrabutylammonium hydrogen sulfate (TBAS), and 40% (vol/vol) acetonitrile at pH 5.8, Buffer B; 50 mM KH2PO4, 8 mM TBAS at pH 5.8. The nucleotides were detected spectrophotometrically.

SUPPLEMENTAL INFORMATION

Supplemental Information includes four figures and can be found with this article online at doi:10.1016/j.cmet.2011.03.006.

ACKNOWLEDGMENTS

We thank Jin Zhang for providing AKAR3 construct, Alexandra Newton for DKAR plasmid, and Keith R. Laderoute for AMPK null MEFs, Mike Begley for providing lentiviral reagents and assistance with establishing stable cell lines, Irimia Daniel and Octavio Hurtado for valuable assistance with microfluidic device microfabrication, the Nikon Imaging Center at Harvard Medical School for imaging assistance, Rebacca Ward, Ken Swanson, and Jason Localsale for critical reading of the manuscript, and members of the Cantley Lab for helpful discussion. This work was supported by National Institutes of Health grants R01-GM56203 and P01-CA120964 to L.C.C., and R00-CA133245 to B.Z.

Received: October 5, 2010
Revised: January 19, 2011
Accepted: February 25, 2011
Published: April 5, 2011

REFERENCES

Allen, M.D., and Zhang, J. (2006). Subcellular dynamics of protein kinase A activity visualized by FRET-based reporters. Biochem. Biophys. Res. Commun. *348*, 716–721.

Boudeau, J., Baas, A.F., Deak, M., Morrice, N.A., Kieloch, A., Schutkowski, M., Prescott, A.R., Clevers, H.C., and Alessi, D.R. (2003). MO25alpha/beta interact with STRADalpha/beta enhancing their ability to bind, activate and localize LKB1 in the cytoplasm. EMBO J. *22*, 5102–5114.

Budinger, G.R., Chandel, N., Shao, Z.H., Li, C.Q., Melmed, A., Becker, L.B., and Schumacker, P.T. (1996). Cellular energy utilization and supply during hypoxia in embryonic cardiac myocytes. Am. J. Physiol. *270*, L44–L53.

Cohen-Saidon, C., Cohen, A.A., Sigal, A., Liron, Y., and Alon, U. (2009). Dynamics and variability of ERK2 response to EGF in individual living cells. Mol. Cell *36*, 885–893.

Dorfman, J., and Macara, I.G. (2008). STRADalpha regulates LKB1 localization by blocking access to importin-alpha, and by association with Crm1 and exportin-7. Mol. Biol. Cell *19*, 1614–1626.

Durocher, D., Taylor, I.A., Sarbassova, D., Haire, L.F., Westcott, S.L., Jackson, S.P., Smerdon, S.J., and Yaffe, M.B. (2000). The molecular basis of FHA domain:phosphopeptide binding specificity and implications for phospho-dependent signaling mechanisms. Mol. Cell *6*, 1169–1182.

Engelman, J.A., and Cantley, L.C. (2010). Chemoprevention meets glucose control. Cancer Prev Res (Phila) *3*, 1049–1052.

Fay, J.R., Steele, V., and Crowell, J.A. (2009). Energy homeostasis and cancer prevention: the AMP-activated protein kinase. Cancer Prev Res (Phila) *2*, 301–309.

Fogarty, S., and Hardie, D.G. (2010). Development of protein kinase activators: AMPK as a target in metabolic disorders and cancer. Biochim. Biophys. Acta *1804*, 581–591.

Geva-Zatorsky, N., Rosenfeld, N., Itzkovitz, S., Milo, R., Sigal, A., Dekel, E., Yarnitzky, T., Liron, Y., Polak, P., Lahav, G., and Alon, U. (2006). Oscillations and variability in the p53 system. Mol. Syst. Biol. *2*, 2006, 0033.

Hardie, D.G. (2007). AMP-activated/SNF1 protein kinases: conserved guardians of cellular energy. Nat. Rev. Mol. Cell Biol. *8*, 774–785.

Hawley, S.A., Boudeau, J., Reid, J.L., Mustard, K.J., Udd, L., Mäkelä, T.P., Alessi, D.R., and Hardie, D.G. (2003). Complexes between the LKB1 tumor suppressor, STRAD alpha/beta and MO25 alpha/beta are upstream kinases in the AMP-activated protein kinase cascade. J. Biol. *2*, 28.

Hawley, S.A., Pan, D.A., Mustard, K.J., Ross, L., Bain, J., Edelman, A.M., Frenguelli, B.G., and Hardie, D.G. (2005). Calmodulin-dependent protein kinase kinase-beta is an alternative upstream kinase for AMP-activated protein kinase. Cell Metab. *2*, 9–19.

Hurley, R.L., Anderson, K.A., Franzone, J.M., Kemp, B.E., Means, A.R., and Witters, L.A. (2005). The Ca2+/calmodulin-dependent protein kinase kinases are AMP-activated protein kinase kinases. J. Biol. Chem. *280*, 29060–29066.

Hutti, J.E., Jarrell, E.T., Chang, J.D., Abbott, D.W., Storz, P., Toker, A., Cantley, L.C., and Turk, B.E. (2004). A rapid method for determining protein kinase phosphorylation specificity. Nat. Methods *1*, 27–29.

Kahn, B.B., Alquier, T., Carling, D., and Hardie, D.G. (2005). AMP-activated protein kinase: ancient energy gauge provides clues to modern understanding of metabolism. Cell Metab. *1*, 15–25.

Kunkel, M.T., Toker, A., Tsien, R.Y., and Newton, A.C. (2007). Calcium-dependent regulation of protein kinase D revealed by a genetically encoded kinase activity reporter. J. Biol. Chem. *282*, 6733–6742.

Laderoute, K.R., Amin, K., Calaoagan, J.M., Knapp, M., Le, T., Orduna, J., Foretz, M., and Viollet, B. (2006). 5′-AMP-activated protein kinase (AMPK) is induced by low-oxygen and glucose deprivation conditions found in solid-tumor microenvironments. Mol. Cell. Biol. *26*, 5336–5347.

Lage, R., Diéguez, C., Vidal-Puig, A., and López, M. (2008). AMPK: a metabolic gauge regulating whole-body energy homeostasis. Trends Mol. Med. *14*, 539–549.

McDonald, J.C., Duffy, D.C., Anderson, J.R., Chiu, D.T., Wu, H., Schueller, O.J., and Whitesides, G.M. (2000). Fabrication of microfluidic systems in poly(dimethylsiloxane). Electrophoresis *21*, 27–40.

McGee, S.L., and Hargreaves, M. (2008). AMPK and transcriptional regulation. Front. Biosci. *13*, 3022–3033.

Mihalcescu, I., Hsing, W., and Leibler, S. (2004). Resilient circadian oscillator revealed in individual cyanobacteria. Nature *430*, 81–85.

Nagai, T., Yamada, S., Tominaga, T., Ichikawa, M., and Miyawaki, A. (2004). Expanded dynamic range of fluorescent indicators for Ca(2+) by circularly permuted yellow fluorescent proteins. Proc. Natl. Acad. Sci. USA *101*, 10554–10559.

Oakhill, J.S., Chen, Z.P., Scott, J.W., Steel, R., Castelli, L.A., Ling, N., Macaulay, S.L., and Kemp, B.E. (2010). β-Subunit myristoylation is the gatekeeper for initiating metabolic stress sensing by AMP-activated protein kinase (AMPK). Proc. Natl. Acad. Sci. USA *107*, 19237–19241.

Sanders, M.J., Grondin, P.O., Hegarty, B.D., Snowden, M.A., and Carling, D. (2007). Investigating the mechanism for AMP activation of the AMP-activated protein kinase cascade. Biochem. J. *403*, 139–148.

Shaw, R.J., Kosmatka, M., Bardeesy, N., Hurley, R.L., Witters, L.A., DePinho, R.A., and Cantley, L.C. (2004). The tumor suppressor LKB1 kinase directly activates AMP-activated kinase and regulates apoptosis in response to energy stress. Proc. Natl. Acad. Sci. USA *101*, 3329–3335.

Shaw, R.J., Lamia, K.A., Vasquez, D., Koo, S.H., Bardeesy, N., Depinho, R.A., Montminy, M., and Cantley, L.C. (2005). The kinase LKB1 mediates glucose homeostasis in liver and therapeutic effects of metformin. Science *310*, 1642–1646.

Spencer, S.L., Gaudet, S., Albeck, J.G., Burke, J.M., and Sorger, P.K. (2009). Non-genetic origins of cell-to-cell variability in TRAIL-induced apoptosis. Nature *459*, 428–432.

Stapleton, D., Mitchelhill, K.I., Gao, G., Widmer, J., Michell, B.J., Teh, T., House, C.M., Fernandez, C.S., Cox, T., Witters, L.A., and Kemp, B.E. (1996). Mammalian AMP-activated protein kinase subfamily. J. Biol. Chem. *271*, 611–614.

Steinberg, G.R., and Kemp, B.E. (2009). AMPK in Health and Disease. Physiol. Rev. *89*, 1025–1078.

Suter, M., Riek, U., Tuerk, R., Schlattner, U., Wallimann, T., and Neumann, D. (2006). Dissecting the role of 5′-AMP for allosteric stimulation, activation, and deactivation of AMP-activated protein kinase. J. Biol. Chem. *281*, 32207–32216.

Takanaga, H., Chaudhuri, B., and Frommer, W.B. (2008). GLUT1 and GLUT9 as major contributors to glucose influx in HepG2 cells identified by a high sensitivity intramolecular FRET glucose sensor. Biochim. Biophys. Acta *1778*, 1091–1099.

Turk, B.E., Hutti, J.E., and Cantley, L.C. (2006). Determining protein kinase substrate specificity by parallel solution-phase assay of large numbers of peptide substrates. Nat. Protoc. *1*, 375–379.

Willemse, M., Janssen, E., de Lange, F., Wieringa, B., and Fransen, J. (2007). ATP and FRET—a cautionary note. Nat. Biotechnol. *25*, 170–172.

Woods, A., Cheung, P.C., Smith, F.C., Davison, M.D., Scott, J., Beri, R.K., and Carling, D. (1996). Characterization of AMP-activated protein kinase beta and gamma subunits. Assembly of the heterotrimeric complex in vitro. J. Biol. Chem. *271*, 10282–10290.

Woods, A., Johnstone, S.R., Dickerson, K., Leiper, F.C., Fryer, L.G., Neumann, D., Schlattner, U., Wallimann, T., Carlson, M., and Carling, D. (2003). LKB1 is the upstream kinase in the AMP-activated protein kinase cascade. Curr. Biol. *13*, 2004–2008.

Woods, A., Dickerson, K., Heath, R., Hong, S.P., Momcilovic, M., Johnstone, S.R., Carlson, M., and Carling, D. (2005). Ca2+/calmodulin-dependent protein kinase kinase-beta acts upstream of AMP-activated protein kinase in mammalian cells. Cell Metab. *2*, 21–33.

Zhang, J., Ma, Y., Taylor, S.S., and Tsien, R.Y. (2001). Genetically encoded reporters of protein kinase A activity reveal impact of substrate tethering. Proc. Natl. Acad. Sci. USA *98*, 14997–15002.

Zheng, B., and Cantley, L.C. (2007). Regulation of epithelial tight junction assembly and disassembly by AMP-activated protein kinase. Proc. Natl. Acad. Sci. USA *104*, 819–822.